Terahertz Imaging Through Dust

Zachary R. Spencer, Daniel Heligman, and Rajind Mendis

Riverside Research, 2640 Hibiscus Way, Beavercreek, OH 45431, USA
rmendis@riversideresearch.org

***Abstract*—We experimentally demonstrate that THz imaging can provide virtually unimpaired visibility through a dense dust environment that would otherwise result in zero visibility under conventional optical imaging. This work highlights a technological solution to a long-standing problem experienced by conventional optical imaging in brownout conditions.**

Keywords—terahertz, THz, imaging, dust, brownout

I. Introduction

In clear atmospheric conditions, current optical technologies used for imaging and ranging applications are extremely effective. However, in adverse conditions that comprises of turbid media such as dust, these optical imaging techniques suffer significantly due to the enhanced atmospheric attenuation. The enhanced attenuation is due to the inherent scattering of optical waves by the suspended dust particles having a micron-sized scale that is comparable to or larger than the wavelength of light. In contrast, terahertz (THz) waves will not be subjected to a similar degree of scattering, due to the much longer wavelength, in the range of upwards of hundreds of microns. Therefore, in such adverse atmospheric conditions, THz imaging is expected to be more effective than optical imaging, and may play a pivotal role in designing future outdoor imaging systems for visibility in all atmospheric conditions.

In past years, there have been a few studies investigating the potential of THz imaging in a dust environment. A couple of studies attempted to model the propagation of THz radiation under *brownout* conditions, that is the loss of visibility caused by dust clouds created by the rotor downwash of a helicopter [1, 2]. Then, a very recent purely theoretical study analyzed the THz propagation under dust storm conditions on both Mars and Earth [3]. Another experimental study, albeit looking into wireless data communications, compared the attenuation of THz and infrared signals in dust clouds [4]. Here, we present results of an experimental study investigating the use of broadband THz pulses to image a target through dust.

II. Experiment

The experimental setup is illustrated schematically in Fig. 1 along with photographs of the front view and rear-side view of the actual setup. The THz transceiver consists of a transmitter (Tx) and a receiver (Rx) configured in a colinear reflection geometry. The Tx emits broadband THz pulses, and those that are back-reflected colinear to the transmission axis are detected by the Rx. A THz image of a remote target is created by raster scanning the transceiver and analyzing the pulses reflected off of the target. A custom-made Plexiglass cell is inserted into the THz beam path to create a self-contained chamber that can create an agitated dust environment. We used Chinchilla dust made from 100% natural volcanic mountain pumice to create a suitably dense dust environment. As shown in the schematic of Fig. 1, this dust powder was deposited at the bottom of the sealed Plexi-glass cell, and agitated via a built-in fan with a downward air flow. This scenario emulates a real-world brownout condition that is created by the rotor downwash of a helicopter. As indicated in the schematic, the path length of the THz beam through the chamber is 20 cm, with the target positioned on the opposite side of the chamber, located at the beam focus. As shown in the figure, the target is fabricated by attaching metal tape on a plastic screen to form a cross.

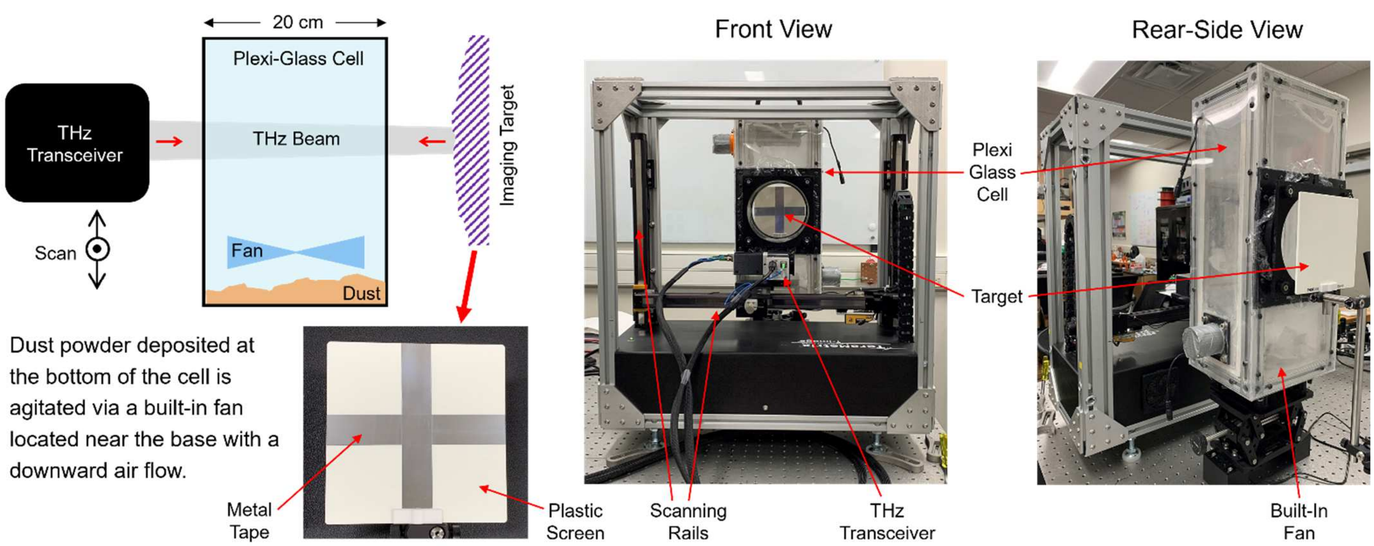

Fig. 1. Schematic of the experimental setup, along with photographs of the actual setup and the imaging target.

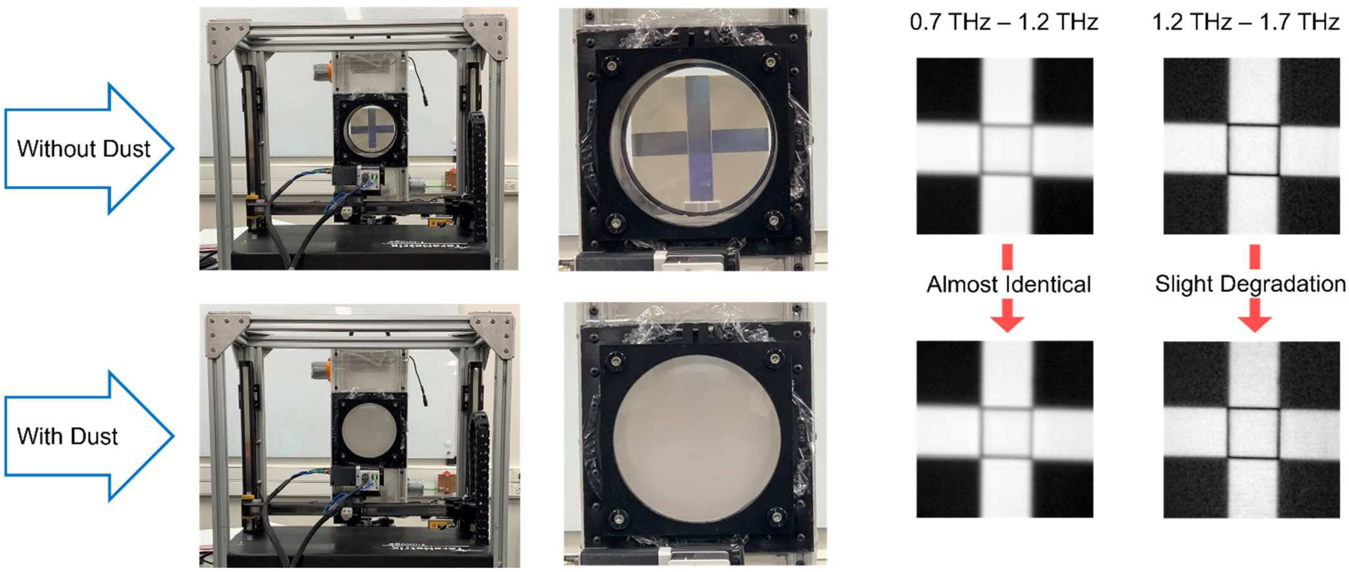

Fig. 2. Top row gives the optical (two left images) and THz images when there is no dust agitated in the cell. The bottom row gives the optical and THz images when dust is agitated in the cell.

To estimate the concentration of dust in the chamber, we carried out a theoretical analysis by computing the total number of dust particles contained within the volume of the chamber. This analysis assumes that the dust particles are uniformly dispersed (via agitation) during the experiment. The average particle size was first estimated by sprinkling some Chinchilla dust onto a glass slide and graphically measuring the particle sizes at various locations of the slide using a calibrated optical microscope. This analysis revealed a wide variation in the particle size, ranging from 15 µm to 200 µm, and a particle concentration of $4\times10^{10}/m^3$ in the cell.

III. Results

Figure 2 presents the imaging results of the experiment that was conducted in two stages. In the first stage, a THz image of the target was created without any dust agitated in the chamber. This is depicted in the top row of the figure, where the target is clearly visible directly through the chamber in the optical photographs. The two THz images (on the right) in grayscale were generated by Fourier-transforming the reflected THz pulses at each pixel and integrating the spectral power from 0.7 THz to 1.2 THz and from 1.2 THz to 1.7 THz. Here, the low-frequency (LF) image has higher signal-to-noise ratio (SNR), but lower resolution, while the high-frequency (HF) image has lower SNR, but higher resolution. For these THz images, the pixel size was 0.5 mm with a 9 cm square grid, and were acquired in 2 minutes and 46 seconds. The light and dark regions in the images correspond to high and low amplitude reflections respectively. The square at the center of the image is due to the overlapping metal tape that is only 60 µm thick, and highlights the depth resolution of the measurement.

In the second stage, the dust was agitated in the chamber by switching on the fan and the same procedure was followed to image the target. This is depicted in the bottom row of the figure, where the target becomes completely invisible through the dust-agitated chamber shown in the photographs. However, in stark contrast, the LF THz image looks almost identical to the one without dust, with the HF THz image only slightly degraded, demonstrating very good visibility through dense dust. This result experimentally confirms the aforementioned theoretical expectation based on scattering losses. The subtle observations in the THz images can be explained by considering the spectra, where the minimal attenuation due to the dust tends to increase as the frequency increases. And since the LF THz images are generated by integrating the spectral power from 0.7 THz to 1.2 THz, a spectral region with negligible attenuation, there is virtually no impact on the image quality.

IV. Conclusions

This proof-of-concept experiment demonstrates the unique ability of THz imaging to provide virtually unimpaired visibility through dense dust that would otherwise result in zero visibility under optical imaging. Thus, this work highlights the means to a technological solution to a long-standing problem experienced by conventional optical imaging in adverse atmospheric conditions. As such, we envision future applications of this technology in aircraft landing systems to overcome brownout conditions, and for the navigation and terrestrial awareness of vehicles used in environments prone to dust storms.

References

[1] C. Prophete, R. Pierrat, H. Sik, E. Kling, R. Carminati and J. de Rosny, "Modeling of an active terahertz imaging system in brownout conditions," Appl. Opt., vol. 57, pp. 6017, 2018.

[2] S. T. Fiorino, J. A. Deibel, P. M. Grice, M. H. Novak, J. Spinoza, L. Owens, and S. Ganti, "A technique to measure optical properties of brownout clouds for modeling terahertz propagation," Appl. Opt., vol. 51, pp. 3605, 2012.

[3] L. T. Wedage, B. Butler, S. Balasubramaniam, Y. Koucheryavy, and M. C. Vuran, "Comparative analysis of terahertz propagation under dust storm conditions on Mars and Earth," IEEE J. Select. Topics Signal Process., vol. 17, pp. 745, 2023.

[4] K. Su, L. Moeller, R. B. Barat, and J. F. Federici, "Experimental comparison of terahertz and infrared data signal attenuation in dust clouds," J. Opt. Soc. Am. A, vol. 29, pp. 2360, 2012.